

Stop Decay into Right-handed Sneutrino LSP at Hadron Colliders

Andre de Gouvêa^a and Shrihari Gopalakrishna^y

Northwestern University, Department of Physics & Astronomy,
2145 Sheridan Road, Evanston, IL 60208, USA.

Werner Porod^z

IFIC - Instituto de Física Corpuscular, CSIC, E-46071 Valencia, Spain.

(Dated: December 24, 2018)

Abstract

Right-handed neutrinos offer us the possibility of accommodating neutrino masses. In a supersymmetric model, this implies the existence of right-handed sneutrinos. Right-handed sneutrinos are expected to be as light as other supersymmetric particles if the neutrinos are Dirac fermions or if the lepton-number breaking scale is at (or below) the supersymmetry (SUSY) breaking scale, assumed to be around the electroweak scale. Depending on the mechanism of SUSY breaking, the lightest right-handed sneutrino may be the lightest supersymmetric particle (LSP). We consider the unique hadron collider signatures of a weak scale right-handed sneutrino LSP, assuming R-parity conservation. For concreteness, we concentrate on stop pair-production and decay at the Tevatron and the Large Hadron Collider, and briefly comment on the production and decay of other supersymmetric particles.

^aElectronic address: degouvea@northwestern.edu

^yElectronic address: shri@northwestern.edu

^zElectronic address: porod@ic.uv.es

I. INTRODUCTION

A renormalizable extension of the standard model (SM) that incorporates neutrino masses can be obtained by introducing (at least two) SM gauge singlet fermions { right-handed neutrinos N_R . Neutrino masses arise due to the fact that right-handed neutrinos can couple to the left-handed ones (ℓ_L) through Yukawa couplings. After electroweak symmetry breaking, the SM neutrinos are endowed with either Majorana or Dirac masses. A supersymmetric version of this scenario implies the existence of new, complex, SM gauge singlet scalar fields { the right-handed sneutrinos \tilde{N}_R .

The right-handed neutrino superfield \hat{N} is a SM gauge singlet and is allowed to have a supersymmetry (SUSY) preserving Majorana mass M_N . In the usual high-scale seesaw mechanism [1], M_N { the scale of lepton number breaking { is, in general, not related to the SUSY breaking scale. It is often considered to be around 10^{14} GeV so that, if the neutrino Yukawa couplings are order one, active neutrino masses are around 0.1 eV, the scale inferred from neutrino oscillation experiments [2]. This scenario, while elegant, is very hard to verify experimentally^y and is motivated by the fact that neutrino Yukawa couplings are "naturally" expected to be of order one. If the seesaw energy scale is indeed very high, right-handed sneutrino masses are expected to be of order M_N and, hence, these are decoupled from low-energy phenomena.

It has recently been emphasized that any value of M_N is technically natural [4] (including $M_N = 0$, in which case the neutrinos are Dirac fermions), and that it is important to explore the phenomenological consequences of all values of M_N . One intriguing possibility is to consider, for example, that the unknown physics of SUSY breaking and lepton number breaking are intimately connected, resulting in a common mass scale. If this is the case (or if the SUSY breaking scale were larger than M_N), right-handed sneutrino masses are expected to be of the same order as the masses of all other superpartners. Finally, the radiative

^y "Sfermions" are, of course, scalar particles, and have no sense of handedness. Throughout, however, we refer to left- and right-handed sfermions (scalar neutrinos, scalar tops, etc), as is commonly done in the literature, in order to indicate the super-partner of the various left- and right-handed chiral fermion fields (the neutrino, the top quark, etc).

^y One possibility is to look for right-handed neutrino traces in the RGE evolution of the Soft SUSY breaking parameters, which could be revealed using precision measurements at a next-generation linear collider [3].

stability of the weak scale indicates that the SUSY breaking scale ought to be around the weak scale, so that super-partners are expected to make their presence felt at TeV scale collider experiments.

Depending on the physics of SUSY breaking, right-handed sneutrino masses may end up below all other "active" super-partner masses, so that the lightest sneutrino is the lightest supersymmetric partner (LSP). In general, left- and right-handed sneutrinos mix. However, given that the seesaw energy scale is assumed to be very low, the neutrino Yukawa coupling is, phenomenologically, required to be very small. Hence, if one assumes that the supersymmetric breaking "A-terms" are proportional to the respective Yukawa couplings, left-right sneutrino mixing is expected to be very small (see, for example, [5] for details, some aspects of which are given in App. A for convenience) and the LSP will turn out to be composed of a mostly right-handed sneutrino, \tilde{N}_R .

In a recent work [5], we considered such a \tilde{N}_R LSP when the Majorana and SUSY breaking mass scales are around the electroweak scale. In this case, the neutrino Yukawa coupling $Y_N \sim 10^{-6}$ in order for the light neutrino masses to be of the order of 0.1 eV. We analyzed the sneutrino sector, pointed out in which cases the left-right sneutrino mixing angle can be tiny resulting in an almost pure \tilde{N}_R LSP, and argued that the \tilde{N}_R is an interesting non-thermal dark matter candidate (see also [6]). In this paper we explore the hadron collider implications of a predominantly \tilde{N}_R LSP. Collider signatures of a mixed \tilde{N}_L – \tilde{N}_R LSP have been explored previously in other studies [7].

Since a weak scale \tilde{N}_R LSP interacts only through the tiny Yukawa coupling Y_N , many unique collider signatures are expected to arise. We will show that the most striking among them is the possibility of the next-to-lightest supersymmetric particle (NLSP) being long-lived enough to leave a displaced vertex in the detector. A similar situation exists in theories of gauge mediation where the gravitino is the LSP [8, 9], with usually the scalar tau or the lightest neutralino as NLSPs. However, the scenario discussed here is distinguished by (a) the potentially long-lived states can be strongly interacting, (b) the LSP carries lepton number, which implies associated leptons in the final state, and (c) the LSP interacts only through the Yukawa coupling Y_N , which generically implies non-universal rates for e, μ , and τ type leptons.

In order to illustrate the unique collider signatures of a \tilde{N}_R LSP, we consider in detail the case where the right-handed stop (\tilde{t}_R) is the NLSP^z, and analyze its pair-production and decay. While serving to illustrate many of the unique features of a \tilde{N}_R LSP, a light stop is natural in many scenarios [10] and is favored in successful theories of electroweak baryogenesis [11]. Stops, being strongly interacting particles, are also expected to be produced at significant rates at the Tevatron and the LHC. Stop production and decay have also been analyzed in other contexts [8, 12, 13].

The outline of the paper is as follows: In Sec. II, we compute the decay rate of the \tilde{t}_R into the 3-body final state $b^+ \tilde{N}_R$. We incorporate this decay matrix element into the Monte Carlo program Pythia (version 6.327) [14] and study the Tevatron and LHC signatures in Sec. III. In Sec. IV, we briefly discuss the dominant signatures of other SUSY NLSP candidates, such as gluinos, sbottoms, gauginos, and sleptons, and comment on “co-LSP” right-handed sneutrinos. We offer our conclusions in Sec. V. The details of the model with which we work were spelled out in detail in [5], and are summarized in App. A. The exact expression for the stop decay matrix element is given in App. B.

II. \tilde{t}_R DECAY TO \tilde{N}_R

In the scenario of interest, assuming R-parity conservation, all supersymmetric particles eventually cascade-decay to the stable \tilde{N}_R LSP. Since the \tilde{N}_R couples only via the tiny Y_N , the NLSP can be potentially long-lived. To illustrate this aspect, in this section we consider in detail the decay of the right-handed stop (\tilde{t}_R). This will be particularly relevant when the \tilde{t}_R is not too heavy, in which case its production cross-section can be large enough to be observable at the Tevatron or the LHC. A brief discussion of the decays of other NLSP candidates is given in Sec. IV. We omit, for simplicity, stop mixing. We find that the inclusion of left-right scalar top mixing does not change significantly any of our results.

Fig. 1 shows the dominant contribution to the decay of a predominantly right-handed stop, which is assumed to be the NLSP, into a pure \tilde{N}_R LSP. The related mode $\tilde{t} \rightarrow t \tilde{N}_R$

^z For simplicity we will take the light \tilde{t} to be predominantly \tilde{t}_R . While stop mixing is, in general, not negligible, we find that its inclusion does not change, qualitatively, any of our results.

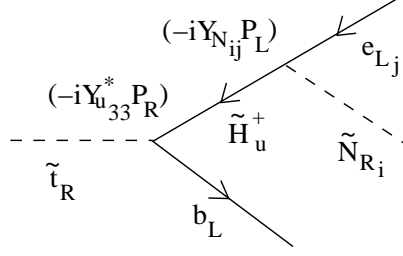


FIG. 1: $\tilde{t}_R \rightarrow b \tilde{N}_R$ decay mode. The arrows indicate fermion number flow.

can also be relevant if kinematically allowed, although phase-space suppressed with respect to $\tilde{t} \rightarrow b \tilde{N}_R$ due to the top quark in the final state.

The complete expression for the lightest stop decay matrix element, including the mixings of all relevant SUSY particles, is presented in App. B. For a purely right-handed stop and sneutrino, in the limit of pure higgsino \tilde{H}^+ exchange^x, the formula for the stop decay width has a simple form. In the \tilde{t}_R rest frame, defining θ_b as the angle between the bottom quark and the charged lepton, the matrix element squared is given by

$$|\mathcal{M}_{fi}|^2 = \frac{4 Y_t^2 Y_N^2 M_{\tilde{t}_R}^2 E_b E_\ell (1 + \cos \theta_b)}{(p_{\tilde{t}_R} \cdot k_b)^2 M_{\tilde{H}^+}^2} : \quad (1)$$

Here, Y_t (Y_N) is the top (neutrino) Yukawa coupling, E_b (E_ℓ) is the b-quark (charged lepton) energy, while k_b is the b-quark four-momentum. $M_{\tilde{t}_R}$ and $p_{\tilde{t}_R}$ are, respectively, the \tilde{t}_R mass and four-momentum, while $M_{\tilde{H}^+}$ is the Higgsino mass. Due to the $(1 + \cos \theta_b)$ factor, the matrix element peaks when the b-quark and the charged lepton are aligned. Later (Sec. III), we will point out that this $\cos \theta_b$ behavior can be used to distinguish between $\tilde{t}_R \rightarrow b \tilde{N}_R$ and $t \rightarrow b W \rightarrow b \ell^+$. It turns out that, for top quark decays, there is no peak in the event distribution when the b-quark and the charged lepton are aligned (cf Fig. 7).

The decay rate is given by

$$\Gamma = 4 Y_t^2 Y_N^2 \frac{M_{\tilde{t}_R}^5}{M_{\tilde{H}^+}^4} \frac{4}{(16\pi^2)^2} \hat{F}_{3PS} ; \quad (2)$$

where \hat{F}_{3PS} is a dimensionless 3-body phase space function. Note that $M_{\tilde{H}^+} > M_{\tilde{t}_R}$.

^x We end that, for the intentions of this paper, it is safe to ignore higgsino-gaugino mixing.

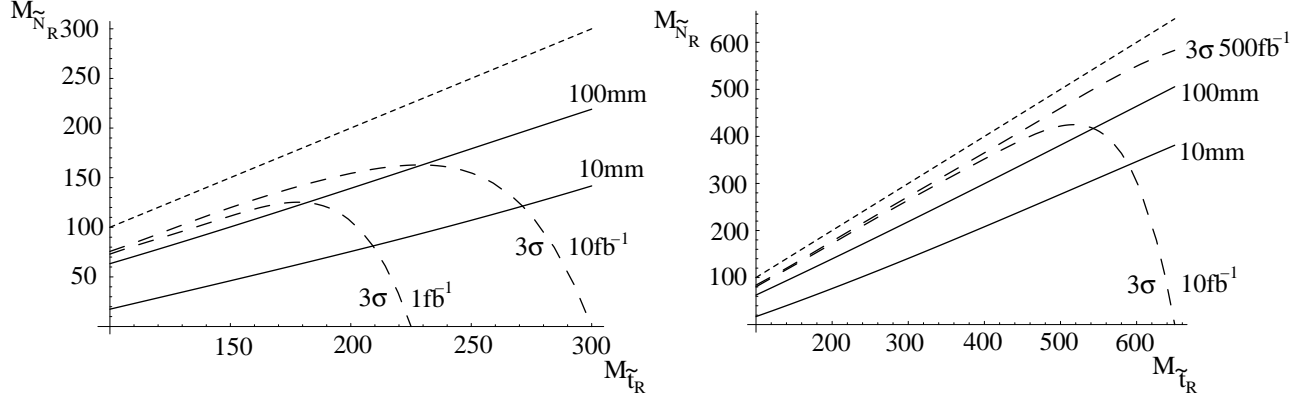


FIG. 2: SOLID { Contours of constant c for the right-handed stop, in the $M_{\tilde{t}_R}$ - $M_{\tilde{N}_R}$ plane. We assume $M_{H^\pm} = 1.1M_{\tilde{t}_R}$. The $M_{\tilde{t}_R} = M_{\tilde{N}_R}$ dotted line bounds the region of parameter space where \tilde{N}_R is the LSP. DASHED { 3σ sensitivity for stop pair production at the Tevatron (left) and the LHC (right), for different integrated luminosities. Note that the displaced vertices are not taken into account when defining the sensitivity. See text for the details.

Num erically, for $M_{\tilde{N}_R} = 100 \text{ GeV}$,

$$c \approx 10 \text{ mm} \frac{4 \cdot 10^{6 \pm 2}}{Y_N} \frac{225 \text{ GeV}^{\pm 5}}{M_{\tilde{t}_R}} \frac{M_{H^\pm}^4}{250 \text{ GeV}} \frac{0.05^{\pm 1}}{\hat{f}_{3PS}} : \quad (3)$$

We remind the reader that \hat{f}_{3PS} is a function of $M_{\tilde{N}_R}$, $M_{\tilde{t}_R}$, and M_{H^\pm} .

For $Y_N \approx 10^6$, c can vary between a few millimeters to several meters, depending on the stop, sneutrino, and Higgsino masses. c values in the $M_{\tilde{t}_R}$ - $M_{\tilde{N}_R}$ plane are depicted in Fig. 2, assuming that $M_{H^\pm} = 1.1M_{\tilde{t}_R}$. For larger values of the Higgsino mass, the constant c contours move toward the $M_{\tilde{t}_R}$ -axis. Displaced vertices, i.e., $c > 1 \text{ mm}$ are to be expected even for large scalar top masses, while for light enough stops and heavy enough LSPs and Higgsinos the stop may even be collider-stable. We elaborate on these possibilities in the next section.

If lepton number is conserved in nature, $M_N = b_N = c_\nu = 0$ (see App. A), neutrinos are Dirac fermions and, in order to obtain the right order of magnitude for the active neutrino masses, $Y_N \approx 10^{12}$ values are required (cf Eq. (A 2)). In this case, c is measured in kilometers and, as far as collider phenomenology is concerned, the \tilde{t}_R is absolutely stable.

Heavy, strongly interacting, collider-stable SUSY particles are expected to form R-

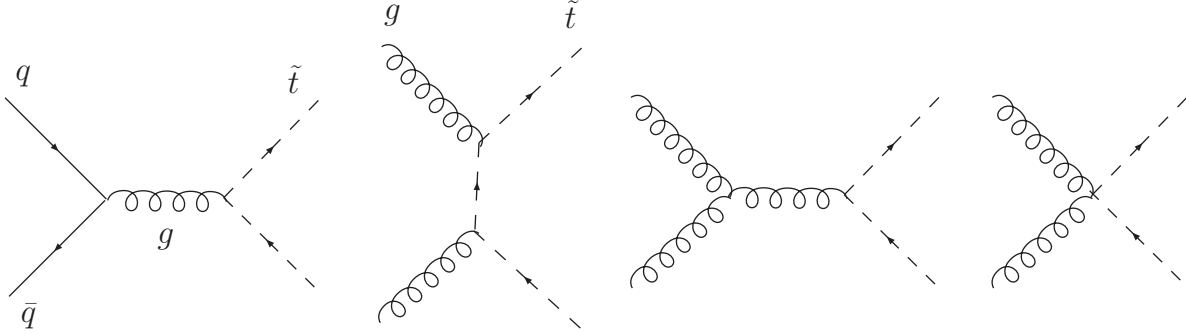


FIG. 3: Dominant parton level \tilde{t} pair-production processes at a hadron collider. The diagrams with gluons in the initial state dominate at the LHC.

hadrons,[†] which behave like heavy nucleon-like objects. Similar experimental signatures have been studied elsewhere [15]. We do not pursue other experimental signatures of heavy, long-lived, hadronic states. We would, however, like to comment on the fact that very long-lived \tilde{t}_R could form narrow "onium-like" $\tilde{t}_R \tilde{t}_R$ bound states[‡] [17], whose decay may lead to a peak above the continuum background. An investigation of this phenomenon will be left for future work.

III. \tilde{t}_R AT THE TEVATRON AND LHC

We consider the production and decay of a \tilde{t}_R NLSP at the Tevatron and the LHC followed by its subsequent decay into a purely right-handed sneutrino \tilde{N}_R LSP, i.e., $\tilde{t}_R \rightarrow b^+ \tilde{N}_R$. Unless noted otherwise, we assume that the \tilde{t}_R decays in this way 100% of the time. To illustrate the behavior of various observables, we will consider the case $M_{\tilde{t}_R} = 225 \text{ GeV}$, $M_{\tilde{N}_R} = 100 \text{ GeV}$, $M_H = 250 \text{ GeV}$, $Y_N = 4 \times 10^{-6}$. In this case, $c \approx 10 \text{ mm}$ (see Eq. 3)).

Fig. 3 depicts the dominant production mechanism of a \tilde{t}_R pair, at leading order. The dominant contribution to \tilde{t}_R decay is depicted in Fig. 1. The \tilde{N}_R escapes the detector as missing energy so that, experimentally, one should observe $pp(p) \rightarrow \tilde{t}_R \tilde{t}_R \rightarrow b^+ b^- +$

[†] The same would also be true of long-lived, gluino bound states [16].

Depending on the details of the SUSY spectrum, there may be other \tilde{t}_R production channels, including gluino pair production, followed by $\tilde{g} \rightarrow t \tilde{t}_R$ (if kinematically accessible). Here we concentrate on "direct" QCD production.

TABLE I: "Level 1" cuts imposed in our analysis. We define $R_b^2 = (b_x)^2 + (b_y)^2$.

1.	Rapidity cuts	$ j , j_b < 2.5$
2.	p_T cuts	$p_{T,j} > 20 \text{ GeV}, p_{T,b} > 10 \text{ GeV}$
3.	Isolation cut	$R_b > 0.4$

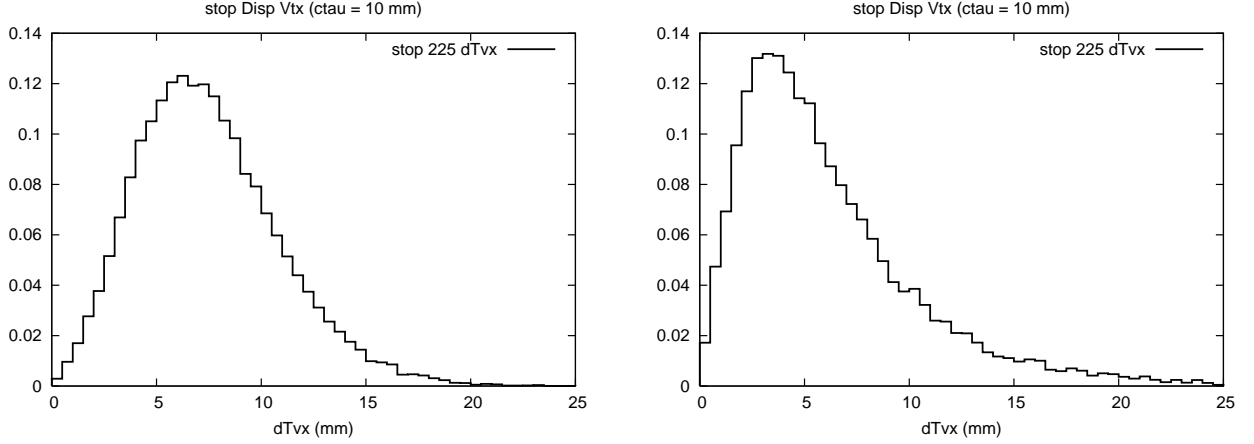


FIG. 4: The distributions of the transverse displacement of the stop (in mm), at the Tevatron (left) and the LHC (right).

E_T . The dominant physics background for this process is expected to be top quark pair production: $pp(p) \rightarrow t\bar{t} \rightarrow bW^+bW^- \rightarrow b^+b^- + E_T$, where the missing energy is due to neutrinos in the final state. We use the Monte Carlo program Pythia (version 6.327) in order to analyze, at the parton level, the signal and background at the Tevatron and the LHC.

The observables available in order to discriminate the signal from background are the transverse components of k_b, k_{b^+}, k_{b^-} and k_ν . We impose the "level 1" cuts shown in Table I, necessitated by the detector geometric acceptance and thresholds. For the isolation cut, we make the standard definition $R_b^2 = (b_x)^2 + (b_y)^2$. These values are typical of other Tevatron analyses, and are meant to approximate the capabilities of the LHC detectors.

Fig. 4 depicts the resulting transverse displacement (in the $x-y$ plane), after including the boost of the stop at the Tevatron (left) and the LHC (right). Even though the stop is more boosted at the LHC (compared to the Tevatron) due to the higher center-of-mass energy, the stop pair is more forward peaked at the LHC, causing their transverse displacement to

be smaller at the LHC (compared to the Tevatron). For other M_{N_R} and M_{t_R} values, the transverse displacement scales with the scalar top's c . These have been discussed in the previous section, and are depicted in Fig. 2.

If a stop is long-lived enough, it will behave like a stable or quasi-stable hadronic object (as commented on earlier). If it decays before exiting the tracking subsystem, a displaced vertex may be reconstructed through the stop decay products' 3-momentum meeting away from the primary interaction point. In the example considered, a displaced vertex of 10 mm can be easily discerned at the Tevatron and the LHC. On each side, the b-quark itself leads to an additional displaced vertex, and its 3-momentum vector can be reconstructed from its decay products. In combination with the 3-momentum of the lepton, the stop displaced vertex can be determined. In order to reveal the displaced vertex, one must require either the b-quark or the charged lepton 3-momentum vector to miss the primary vertex. Since a pair of stops is produced, we would expect to discern two displaced vertices in the event (not counting the displaced vertices due to the b-quarks). If a b-quark ($^+$) cannot be distinguished from a b-antiquark ($^-$), the associated combinatoric problem of assigning the decay products to the parent stop will have to be considered. Such an event with two displaced vertices is quite uncommon in SUSY models^y and might prove to be one of the main distinguishing characteristics of such a scenario. A cut on the displaced vertex provides for a very effective way to separate stop events from the top background. If one can efficiently explore such cuts, we anticipate that NLSP scalar top searches may turn out to be physics-background free.

Another characteristic feature is the non-universal rates for decays into e , μ , and τ leptons. This is to be expected given that the stop decays are proportional to the Y_N 's which are in general different for the three leptons. Here, we do not take advantage of this feature.

If the stop displaced vertex cannot be efficiently resolved, one will have to resort to more conventional analysis methods. In the remainder of this section, we explore various kinematical distributions for both the signal (right-handed scalar top pair production) and the physics background (top pair production), obtained after imposing the level 1 cuts listed

^y Other models with this feature are the NMSSM with a singlino LSP [21], and the case of bilinear R-parity breaking where neutrino masses are generated via R-parity breaking effects [22].

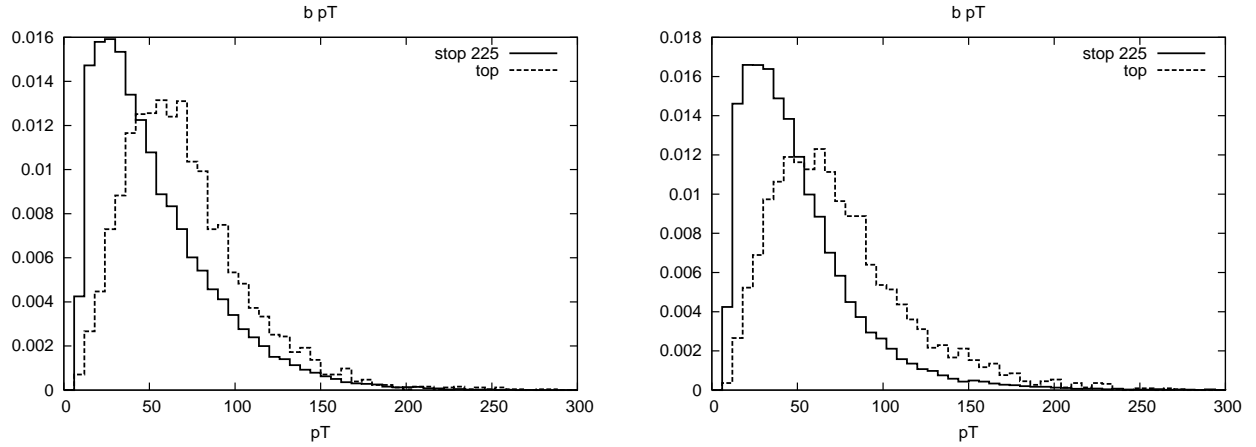


FIG. 5: The distribution of p_T of the b-quark at the Tevatron (left) and LHC (right) resulting from the decay of a 225 GeV stop and a top quark.

in Table I. All the distributions are in the lab frame, normalized to unit area. Note that the analysis performed here also applies to other SUSY scenarios in which the scalar top decays predominantly to bottom plus charged lepton plus missing energy, regardless of whether the stop decays promptly or leaves behind a displaced vertex.

Fig. 5 depicts the parton level distributions of the p_T of the b-quark at the Tevatron (left) and the LHC (right) resulting from a 225 GeV stop and from a top, obtained using Pythia. Fig. 6 depicts the distributions of the p_T of the charged lepton at the Tevatron (left) and the LHC (right), resulting from a 225 GeV stop, and from a top. The p_T of the b-quark from the 225 GeV stop peaks at a lower value compared to the top quark background, and therefore accepting them at high efficiency for $p_T < 40$ GeV will be very helpful in maximizing the signal acceptance. The signal and background shapes are quite similar and no simple set of p_T cuts can be made in order to significantly separate signal from background. As the mass difference between the \tilde{t}_R and the N_R decreases, the b-quark and the charged lepton p_T distributions peak at lower values due to less available phase-space, making the measurements more challenging.

Fig. 7 depicts the distribution of $\cos \theta_b$, the angle between the 3-momenta k_b and k_ℓ , for both the signal and background. It is important to appreciate that, by default, Pythia generates stop decays into the 3-body final state according only to phase-space, ignoring

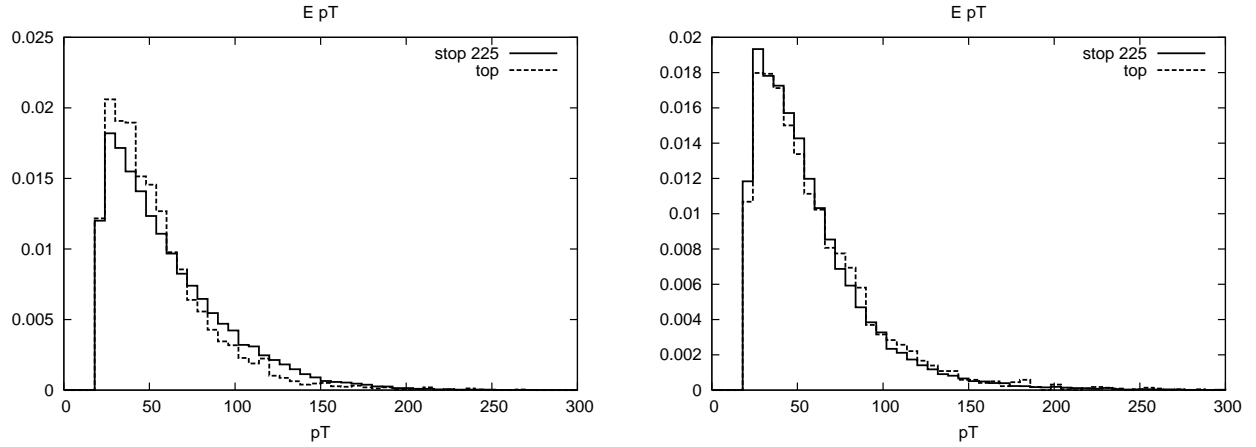


FIG . 6: The distribution of p_T of the charged lepton resulting from the decay of a 225 GeV stop, and a top, at the Tevatron (left) and the LHC (right).

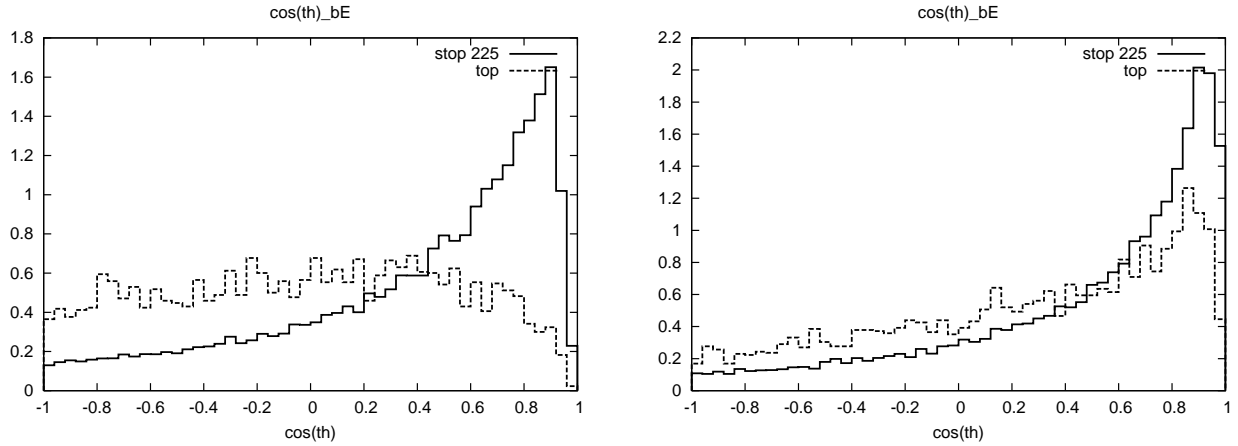


FIG . 7: The distribution of $\cos \theta_b$, resulting from the decay of a 225 GeV stop, and a top, at the Tevatron (left) and LHC (right).

the angular dependence of the decay matrix element. We have reweighted Pythia events to include the correct angular dependence in the decay matrix element. Consistent with the expectation from Eq. (1), we see for the signal that the distribution peaks for the b-quark and charged lepton 3-momenta aligned, unlike the background.² It is unfortunate that the isolation level cut (see Table I) on the leptons removes more signal events than background

² For another discussion on how to extract stop NLSP's (in a different context) see [8].

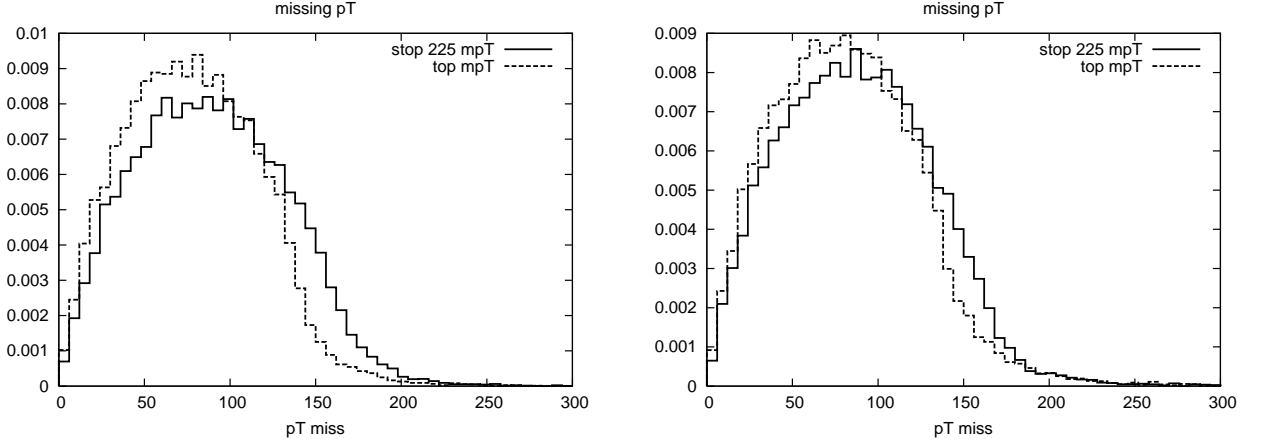


FIG. 8: The total \not{p}_T distribution resulting from a 225 GeV stop, and a top, at the Tevatron (left) and the LHC (right).

events. Relaxing this constraint as much as practical would help in this regard.

Fig. 8 shows the total \not{p}_T distribution resulting from the production and decay of a 225 GeV stop and a top quark for the Tevatron (left) and the LHC (right). Here \not{p}_T is defined as $\sqrt{\not{p}_{Tx}^2 + \not{p}_{Ty}^2}$, with \not{p}_{Tx} and \not{p}_{Ty} the x and y components of the total missing momentum vector. Pythia ignores the spin correlation between the two opposite side particles and therefore the \not{p}_T distributions shown are not entirely accurate in case of the t-quarks. However, spin correlation modifies the \not{p}_T distribution to only a small degree [18], although it can lead to significant effects in suitably chosen observables [19].

The angular correlation of the stop pair is different from that of the top quark pair, since the former is a scalar and the latter a fermion. We expect the quantities $k_{b\rightarrow j}$ and $k_{\bar{b}\rightarrow \bar{j}}$ to inherit some of this difference, making these potentially good discriminants for signal and background. As just mentioned, Pythia is not suitable to investigate this aspect since it does not retain spin correlations, and we postpone this investigation to future work.

The sensitivity of the Tevatron and the LHC to the stop NLSP is depicted in Table II and Table III, respectively, for various \tilde{t}_R and \tilde{N}_R masses. The stop pair-production cross-section from Pythia multiplied by the appropriate K-factor [20] is displayed in the table for the Tevatron and the LHC, along with the top pair-production cross-section [25]. The fraction of signal events that passes level 1 cuts (specified in Table I), denoted ϵ , obtained

TABLE II: Signal (stop) and background (top) pair production cross-section at the Tevatron, with $\mu_b = 0.5$, and $\mu_s = 0.9$. σ_s and σ_B denote the signal and background cross-sections, f the fraction that passes level 1 cuts (see Table I), S and B the number of signal and background events for 1 fb^{-1} .

$M_{t\bar{t}}$	M_{N_R}	σ_s (pb)	σ_B (pb)	f	S	B	$S=B$	$S=\frac{P}{B}$	$S=\frac{P}{S+B}$
100	50	11.83	6.77	0.26	162	9	18.93	55.36	12.4
	75	11.83	6.77	0.04	4	9	0.45	1.31	1.09
150	100	1.24	6.77	0.29	21	9	2.46	7.21	3.87
	125	1.24	6.77	0.05	1	9	0.07	0.21	0.21
175	100	0.48	6.77	0.47	22	9	2.53	7.39	3.93
	150	0.48	6.77	0.05	0.2	9	0.03	0.08	0.08
250	100	0.04	6.77	0.71	4	9	0.48	1.4	1.15
	200	0.04	6.77	0.31	1	9	0.09	0.27	0.26

TABLE III: Signal (stop) and background (top) pair production cross-section at the LHC, with $\mu_b = 0.5$, and $\mu_s = 0.9$. σ_s and σ_B denote the signal and background cross-sections, f the fraction that passes level 1 cuts (see Table I), S and B the number of signal and background events for 10 fb^{-1} .

$M_{t\bar{t}}$	M_{N_R}	σ_s (pb)	σ_B (pb)	f	S	B	$S=B$	$S=\frac{P}{B}$	$S=\frac{P}{S+B}$
100	75	1332.5	873	0.03	1938	8662	0.22	20.82	18.82
	83	1332.5	873	0.01	73	8662	0.01	0.78	0.78
150	100	228.79	873	0.23	25325	8662	2.92	272.1	137.37
	128	228.79	873	0.02	144	8662	0.02	1.54	1.53
250	200	21.32	873	0.26	2886	8662	0.33	31.01	26.86
	225	21.32	873	0.03	40	8662	0.01	0.43	0.43
500	400	0.56	873	0.59	398	8662	0.05	4.28	4.19
	425	0.56	873	0.48	263	8662	0.03	2.83	2.78
650	250	0.14	873	0.83	195	8662	0.02	2.10	2.08
	500	0.14	873	0.71	145	8662	0.02	1.56	1.54

using Pythia is shown, and the fraction of background events (not shown in the table) is 0.79 (Tevatron), and 0.7 (LHC). We compute the number of signal events (S), background events (B), for 1 fb^{-1} (Tevatron) and 10 fb^{-1} (LHC), and compute the figures-of-merit S/B , $S = \frac{P}{B}$ and $S = \frac{P}{S+B}$. We have taken the b -tagging efficiency $\epsilon_b = 0.5$ and the lepton identification efficiency $\epsilon_\ell = 0.9$. The number of events is given by $N = L \cdot \sigma_b^2$, where L is the integrated luminosity. It is important to emphasize that we do not consider the possibility that one can efficiently identify that the scalar top decays far from the production point. If this is the case, we anticipate that physics backgrounds will be significantly reduced. At the same time, we remind the reader that we have fixed $M_{\tilde{t}_R} = M_{\tilde{t}_R} = 1:1$. For larger values of this ratio, scalar tops are expected to be (much) longer-lived, in which case other approaches to data analysis are required.

Fig. 2 shows the projected 3 σ contours in the $M_{\tilde{t}_R} - M_{\tilde{N}_R}$ plane, with 1 and 10 fb^{-1} at the Tevatron, and 10 and 500 fb^{-1} at the LHC. We find from our analysis with just level 1 cuts (see Table I) that the Tevatron can probe stop masses up to about 300 GeV (with 10 fb^{-1}), while the LHC reach extends slightly above 650 GeV (with 500 fb^{-1}), with the reach depending on the \tilde{N}_R mass. We expect that the sensitivity can be improved with more sophisticated cuts and a multivariate analysis. A smaller $M_{\tilde{t}_R} - M_{\tilde{N}_R}$ mass difference leads to softer b -quarks and charged leptons, resulting in a smaller ϵ and leading to a lower statistical significance. Here we assume that the stop decays to the leptonic channel considered with 100 % branching ratio. In a specific model the actual significance can be obtained by including the branching ratio. Our estimates for the top and stop production rates are in good qualitative agreement with experimental measurements of top production [23] and bounds imposed by stop searches at the Tevatron [24].

IV. PRODUCTION AND DECAY OF OTHER SUSY PARTICLES

In this section we briefly discuss some aspects of unique signatures associated with the production and decay of other SUSY particles. The actual signatures depend on the detailed SUSY spectrum. In particular, we digress on features associated with other NLSP candidates, including sbottoms, gluinos, gauginos and sleptons. We also comment on the fate of the "other" mostly right-handed sneutrinos, which are expected to be, as far as

collider experiments are concerned, also stable.

A . sbottom

If the \tilde{b}_R is the NLSP, its pair-production cross-section is naively similar to the stop NLSP case discussed in Sec. III. The decay channel analogous to the one discussed for the stop NLSP is $\tilde{b} \rightarrow t \tilde{N}_R$. This decay channel, however, may not be kinematically accessible. Regardless, the dominant channel for a large chunk of the parameter space is expected to be $\tilde{b}_R \rightarrow b \tilde{N}_R$, resulting in the signature $pp(p) \rightarrow bb + \cancel{E}_T$. Due to the additional suppression of the decay rate by Y_b^2 , we expect NLSP sbottoms to be more long-lived than the stop NLSP by a factor of Y_t^2/Y_b^2 . Here, we expect that it will be harder (compared to the \tilde{t}_R NLSP case) to identify efficiently a potentially displaced vertex, due to the absence of charged leptons in the final state. One may be able to achieve this by asking whether the reconstructed 3-momenta of the opposite side b-quarks point back to the primary vertex. One source of background is QCD bb production { huge { but demanding substantial \cancel{E}_T should help extract the signal. We expect that substantial \cancel{E}_T will also be crucial for triggering on the event.

The decay mode $\tilde{b}_R \rightarrow c \tilde{N}_R$ is suppressed by $|V_{cb}|^2$ compared to the mode discussed above, and should have a branching ratio around 10^{-3} . This mode leads to the signature $pp(p) \rightarrow cc^{*+} \cancel{\nu} + \cancel{E}_T$. The additional pair of leptons will help in discriminating these events from background but, given the small branching ratio, we expect this decay mode to be out of the reach of the Tevatron (but not the LHC). As with stop NLSPs, given that the decay is proportional to the Y_N 's, we generically expect different rates for different charged lepton final states as a characteristic of this scenario.

B . Gluino

If the gluino is the NLSP, it decays primarily to a four-body final state $\tilde{g} \rightarrow qq^{0*+} \tilde{N}_R$, via on-shell q^0 and $\tilde{\nu}^+$. This leads to the signature $pp(p) \rightarrow 4j + 2\cancel{\nu} + \cancel{E}_T$. A related mode is to a neutrino in the final state, i.e., $\tilde{g} \rightarrow qq \tilde{N}_R$ via on-shell q and $\tilde{\nu}^0$, leading to the signature

$pp(p) \rightarrow 4j + E'_T$. Unlike the previous mode, in this mode the leptons are unobservable.

Owing to the four-body final state and the Y_N suppression, the gluino is expected to be quite long lived. The decay rate is

$$\Gamma_g = \frac{1}{2} g^2 Y_N^2 \frac{M_g^7}{M_H^2 M_g^4} \frac{4}{(16\pi^2)^3} \hat{f}_{4PS}^g; \quad (4)$$

where \hat{f}_{4PS} is a dimensionless four-body phase-space function. Compared to the \tilde{t}_R NLSP decay width (Eq. 2),

$$c_g = c_{\tilde{t}_R} 10^4 \frac{M_{\tilde{t}_R} M_g}{M_H M_g} \frac{\hat{f}_{3PS}^{\tilde{t}_R}}{\hat{f}_{4PS}^g}; \quad (5)$$

We naively estimate $c_g > 10^4 c_{\tilde{t}_R}$, so that, for all practical collider purposes, the gluino is stable ($c > 100$ m). Such a long lived gluino forms an R-hadron and some of its experimental signatures have been discussed in [15].

As an aside, we comment that if the mass spectrum is such that the gluino is no longer so long lived, the fact that the gluino is a Majorana particle can be used in order to identify gluino production and decay. Such processes can result in decays into a pair of same-sign leptons, and, if kinematically accessible, the case of decays into same-sign tops can be easily distinguished from background [13].

C. Charginos

Charginos can be pair-produced via o -shell and Z -boson exchange, and the NLSP chargino decays into the LSP via $\tilde{\chi}^+ \rightarrow \tilde{\chi}^0 \tilde{N}_R$. This leads to the signature $pp(p) \rightarrow \tilde{\chi}^+ \tilde{\chi}^- + E'_T$. The production cross-section is suppressed relative to that of strongly interacting SUSY particle pair production by $(g=g_s)^4 \sim 10^{-2}$, and therefore probably too small to be probed at the Tevatron. The LHC, on the other hand, will have the ability to produce weakly interacting states in significant numbers. The chargino lifetime can be easily estimated as

$$\Gamma_H = Y_N^2 M_H \frac{4}{16\pi^2} \hat{f}_{2PS}^H; \quad (6)$$

where \hat{f}_{2PS} is a dimensionless two-body phase-space function. Comparing this with the stop NLSP decay width (Eq. 2), we obtain

$$c_H = c_{\tilde{t}_R} \frac{M_{\tilde{t}_R}}{M_H} \frac{1}{16\pi^2} \frac{\hat{f}_{3PS}^{\tilde{t}_R}}{\hat{f}_{2PS}^H}; \quad (7)$$

For $M_{H^\pm} = 1.1 M_{\tilde{\tau}_R}$, $\hat{f}_{2PS} \approx 0(1)$, and our numerical estimate $\hat{f}_{3PS} \approx 0.05$, we get $c_{H^\pm} c_{\tilde{\tau}_R} \approx 10^{-4}$. Chargino decay is, as far as hadron collider experiments are concerned, prompt. The main background is expected to be W -boson pair production.

Neutralinos can be pair-produced via an o -shell squark, and an NLSP neutralino decays, most of the time, invisibly: $\tilde{\chi}^0 \rightarrow \tilde{N}_R$. A gluon jet or photon can be radiated from the initial state leading to the signature $pp(p) \rightarrow j\cancel{E}_T$ or \cancel{E}_T . Due to the electroweak production cross-section, it is unlikely that such processes are accessible at the Tevatron. At the LHC, on the other hand, one may run into a large number of these events. Whether or not these can be extracted from the various backgrounds requires a dedicated study, beyond the ambitions of this brief section.

D. Slepton

Sleptons are pair produced by the exchange of virtual \tilde{g} and Z -boson exchange, followed by the decay $\tilde{\ell} \rightarrow \ell \tilde{N}_R$. This leads to the signature $pp(p) \rightarrow \ell^+ \ell^- + \cancel{E}_T$. Since this is a three-body decay, like in the case of the stop NLSP, we expect displaced vertices or very long-lived sleptons. The only observable decay product of the NLSP slepton is the charged lepton, so the displaced vertex is characterized by a lepton track that does not point back to the primary vertex. The dominant background for this channel is W -boson pair production. Note that this case is similar to some manifestations of gauge-mediated SUSY breaking with the gravitino as the LSP and the slepton (usually the scalar tau), as the NLSP [9].

E. Co-LSP right-handed sneutrino

Given that there are at least two generations of right-handed sneutrinos ($\tilde{N}_R^{(i)}$), we explore the possibility of observable consequences of these "co-LSP's." Such a possibility was already raised during studies of the lightest left-handed sneutrino as the LSP [26]. It is possible, in all the decays considered so far, that a heavier co-LSP, say $\tilde{N}_R^{(2)}$, is produced. This state later decays to the "real" LSP, say $\tilde{N}_R^{(1)}$. The relevant (observable) decay channels are $\tilde{N}_R^{(2)} \rightarrow \tilde{N}_R^{(1)} \ell^+ \ell^-$ and the one-loop decay $\tilde{N}_R^{(2)} \rightarrow \tilde{N}_R^{(1)} \gamma$. An estimate of these decay widths

is

$$\begin{aligned} \Gamma_{N_R^{(2)}} &= Y_N^4 \frac{M_{N_R^{(2)}}^3}{M_{\tilde{N}_R}^2} \frac{4}{(16\pi^2)^2} \hat{f}_{3PS}^{\#} ; \\ &= 10^{-26} \text{ eV} \left(\frac{M_{N_R^{(2)}}}{100 \text{ GeV}} \right)^4 \left(\frac{M_{N_R^{(2)}}}{M_{\tilde{N}_R}} \right)^2 \hat{f}_{3PS} \text{ GeV} ; \end{aligned} \quad (8)$$

where \hat{f}_{3PS} is a dimensionless phase space factor. Note that this decay width is proportional to Y_N to the fourth power. This leads to a lifetime well above 1 s, so that $N_R^{(2)}$ is long-lived enough to exit the detector unseen.

A concern for such long lived particles is whether they disrupt the successful predictions of big-bang nucleosynthesis. Note that, if the mass difference between the co-LSP states is relatively small (as one would naively expect), $\hat{f}_{3PS} \approx 1$, and the lifetime may be orders of magnitude longer than the naive estimate above. A more more detailed study, beyond the ambitions of this section, is required in order to determine the impact of these decaying co-LSPs in the early universe.

V. CONCLUSIONS

Right-handed sneutrinos (\tilde{N}_R) are present in a supersymmetric theory that includes right-handed neutrinos. If the right-handed neutrino Majorana mass and the SUSY breaking scale are identified with the electroweak scale, our understanding of light neutrino masses requires the neutrino Yukawa coupling to be $Y_N \approx 10^{-6}$. Depending on the details of the SUSY breaking mechanism, it is possible that a predominantly right-handed sneutrino is the LSP. We detailed such a theory in [5], and explored the cosmological implications of a right-handed sneutrino LSP. In this paper we study some hadron collider (Tevatron and LHC) signatures of such a \tilde{N}_R LSP.

We show that if such a \tilde{N}_R is the lightest supersymmetric particle (LSP), the collider signatures are very interesting, owing to the fact that the \tilde{N}_R interacts only through the tiny Y_N . If R-parity is conserved, all heavier SUSY particles eventually have to cascade decay to the \tilde{N}_R through the interaction parameterized by Y_N . Among other potentially observable effects (leptons, missing energy), we find that the next-to lightest supersymmetric particle (NLSP) is potentially (very) long-lived. If a mostly right-handed sneutrino is the LSP, one

generically expects displaced vertices due to the relatively long NLSP lifetime, or heavy, collider-stable hadronic or weak states.

In order to illustrate these aspects, we consider, in Sec. II, the scalar top 3-body decay $\tilde{t}_R \rightarrow b^+ \tilde{N}_R$ via an on-shell H^\pm . We calculate the decay matrix element showing explicitly the dependence on ϕ_b , the angle between the 3-momenta of the final-state b-quark and charged lepton. We show that for $Y_N \sim 10^{-6}$, c_β for the scalar top varies from millimeters to meters. In addition, since the leptons are produced through the Yukawa couplings Y_N , we expect non-universal rates for the production of e, μ and τ leptons.

We performed a simulation of stop pair production and decay at the Tevatron and the LHC, using the Monte Carlo program Pythia. Pythia by default treats the 3-body final state according only to phase-space, so we modified the program to correctly incorporate the decay matrix element. The signature of this signal is $pp(p) \rightarrow \tilde{t}_R \tilde{t}_R^* \rightarrow b^+ b^- + \cancel{E}_T$. The dominant physics background is top quark pair production $pp(p) \rightarrow t\bar{t} \rightarrow bW^+ bW^- \rightarrow b^+ b^- + \cancel{E}_T$, where the missing energy is due to final state neutrinos.

The transverse displaced vertex after folding in the boost of the stop is shown in Fig. 4, and is easily discernible at the Tevatron and the LHC. This can be used to very effectively suppress the background. If the parameters are such that a displaced vertex cannot be resolved, we will have to rely on the distributions and event rates in order to show an excess above background. We see that the p_T distributions of the b-quark and the charged lepton from a 225 GeV stop and the top background are quite similar, and no clear set of p_T cuts can be applied to separate them. The $\cos \phi_b$ distribution is, however, sufficiently different for signal and background, as can be seen in Fig. 7.

We summarize the Tevatron and LHC reach in Tables II and III. From this physics level study, we estimate that the Tevatron can probe stop masses up to about 300 GeV with 10 fb^{-1} , while the LHC is sensitive to about 650 GeV with 500 fb^{-1} of integrated luminosity. This reach was obtained after applying only the level 1 cuts shown in Table I. A more sophisticated analysis is expected to extend the estimates obtained here. Needless to say, a full detector-level simulation is necessary in order to realistically assess the capabilities of the Tevatron and the LHC. We would like to point out that the results presented in Tables II and III should also apply to other SUSY scenarios in which the scalar top decays

predominantly to a b-jet, a charged lepton, and missing transverse energy, regardless of whether the stop decay occurs promptly or leaves behind a displaced vertex.

Of course, the nature of the NLSP depends on the details of supersymmetry breaking. We offered some remarks in Sec. IV on what channels are promising for several potential NLSP candidates. We leave a comprehensive analysis of any possible cascade decay chains for future work.

Acknowledgments

We thank the organizers and participants of the LC workshop Snowmass 2005, where this work was initiated. We thank Steve Mrenna for discussions, help with Pythia and comments on the manuscript; Peter Skands for discussions and help with Pythia; Marcela Carena, Bob McElrath and Tilman Plehn for discussions; Jon Hays, Victoria Martin, Jason Nielsen, and Reinhard Schienhorst for discussions on experimental issues. The work of AdG and SG is sponsored in part by the US Department of Energy Contract DE-FG 02-91ER 40684, while W P is supported by a MEC Ramón y Cajal contract and by the Spanish grant FPA 2005-01269.

APPENDIX A : THE MODEL

To the field content of the MSSM, we add (for each generation) a right-handed neutrino superfield $\tilde{N} = (\tilde{N}_R; N; F_N)$. Written as left-chiral fields, the superfields are: $\tilde{Q}, \tilde{U}^c, \tilde{D}^c, \tilde{L}, \tilde{E}^c, \tilde{N}^c$. As usual, the MSSM Higgs doublet superfields are \tilde{H}_u and \tilde{H}_d . Here we repeat the main aspects of the model, details of which can be found in [5].

The superpotential is

$$W = \tilde{U}^c Y_U \tilde{Q} \tilde{H}_u - \tilde{D}^c Y_D \tilde{Q} \tilde{H}_d + \tilde{N}^c Y_N \tilde{L} \tilde{H}_u - \tilde{E}^c Y_E \tilde{L} \tilde{H}_d + \tilde{N}^c \frac{M_N}{2} \tilde{N}^c + \tilde{H}_u \tilde{H}_d; \quad (A1)$$

where $A \cdot B$ denotes the antisymmetric product of the fields A and B , Y are the Yukawa couplings that are 3×3 matrices in generation space, and, M_N breaks lepton number.

After electroweak symmetry breaking (when the Higgs scalars get vacuum expectation values v_u and v_d), the lowest neutrino mass eigenvalue is given by the standard seesaw

relation

$$m = \frac{v_u^2 Y_N^2}{M_N}; \quad (\text{A } 2)$$

where we assume $v_u Y_N \ll M_N$. Neutrino oscillation experiments indicate that $m \lesssim 0.1 \text{ eV}$, and if $M_N \gg v$, Eq. A 2) implies that $Y_N \lesssim 10^{-6}$.

The soft SUSY breaking Lagrangian is given by

$$\begin{aligned} \mathcal{L}_{\text{SUSY Br}} = & \tilde{g}_1^2 m_q^2 \tilde{Q}_L^2 + \tilde{g}_2^2 m_u^2 \tilde{u}_R^2 + \tilde{g}_3^2 m_d^2 \tilde{d}_R^2 + (\tilde{g}_1^2 A_u \tilde{Q}_L \tilde{u}_R + \tilde{g}_2^2 A_d \tilde{Q}_L \tilde{d}_R + \text{h.c.}) \\ & \tilde{g}_1^2 m_\ell^2 \tilde{L}_L^2 + \tilde{g}_2^2 m_N^2 \tilde{N}_R^2 + \tilde{g}_3^2 m_e^2 \tilde{e}_R^2 + (\tilde{g}_1^2 A_N \tilde{L}_L \tilde{N}_R + \tilde{g}_2^2 A_e \tilde{L}_L \tilde{e}_R + \text{h.c.}) \\ & + (\tilde{\nu}_L \tilde{u}_R)^T \frac{C_\nu}{2} (\tilde{\nu}_L \tilde{u}_R) + \tilde{N}_R^T \frac{b_N M_N}{2} \tilde{N}_R + \text{h.c.} \\ & + (b \tilde{h}_u \tilde{d}_R + \text{h.c.}) ; \end{aligned} \quad (\text{A } 3)$$

where \tilde{g}_i and $b_N M_N$ are SUSY-breaking, lepton-number breaking parameters. As usual, m^2 are SUSY breaking scalar masses squared, A are SUSY breaking A-terms, and b is the SUSY breaking Higgs boson B-term.

After electroweak symmetry breaking, the sneutrino mass matrix (generation structure suppressed) is given by

$$M_{\tilde{\nu}}^2 = \frac{1}{2} \begin{pmatrix} 0 & m_{LL}^2 & m_{RL}^2 & v_u^2 C_\nu & v_u Y_N^y M_N \\ m_{RL}^2 & m_{RR}^2 & v_u M_N^T Y_N & (b_N M_N)^y & 0 \\ v_u^2 C_\nu & v_u Y_N^T M_N & m_{LL}^2 & m_{RL}^{2T} & 0 \\ v_u M_N^y Y_N & b_N M_N & m_{RL}^2 & m_{RR}^2 & 0 \end{pmatrix}; \quad (\text{A } 4)$$

where $m_{LL}^2 = (m^2 + v_u^2 Y_N^y Y_N + \frac{1}{2} D^2)$, $m_{RR}^2 = (M_N M_N + m_N^2 + v_u^2 Y_N Y_N^y)$, $m_{RL}^2 = (v_d Y_N + v_u A_N)$, and $D^2 = (m_{\frac{Z}{2}}^2 = 2) \cos 2\beta$ is the D-term contribution.

The $\tilde{\nu}_L$ - \tilde{N}_R mixing angle is given by (see [5] for details)

$$\tan 2\tilde{\nu} = \frac{2 m_{RL}^2 + v_u M_N^y Y_N}{(m_{LL}^2 - v_u^2 C_\nu) - (m_{RR}^2 - b_N M_N)}; \quad (\text{A } 5)$$

If $A_N \ll Y_N$, as is the case in several popular SUSY breaking scenarios, it is easy to see that $\sin \tilde{\nu} \approx Y_N$. For $Y_N \lesssim 10^{-6}$ { the case of interest here } the mixing angle is tiny, and, as long as $m_{RR}^2 < m_{LL}^2$, the LSP is an almost pure \tilde{N}_R .

APPENDIX B : THE DECAY $\tilde{t}_1 \rightarrow b l^+ \tilde{\nu}_1$

Here, we present formulas for the decay width of the 3-body decay of the stop, $\tilde{t}_1 \rightarrow b l^+ \tilde{\nu}_1$. Although in the main body of the paper we consider the case when $\tilde{\nu}_1 = \tilde{\nu}_1^N$ with $\tilde{\nu}_1 = \tilde{N}_R$ as the LSP, the formulas in this section are valid in general.

The matrix element is given by

$$T_{fi} = \sum_{i=1/2}^X u_b(\mathbf{p}_b) [k_{i1}^t P_L + l_{i1}^t P_R] \frac{1}{\sqrt{p_{\tilde{\nu}_1^+} m_{\tilde{\nu}_1^+}}} (k_{i1} P_R + l_{i1} P_L) v(\mathbf{p}_l); \quad (B1)$$

where

$$\begin{aligned} l_{i1}^t &= g \cos \epsilon V_{i1} - Y_t \sin \epsilon V_{i2}; \quad k_{i1}^t = Y_b \cos \epsilon U_{i2}; \\ l_{i1} &= g \cos \tilde{\epsilon} V_{i1} - Y \sin \tilde{\epsilon} V_{i2}; \quad k_{i1} = Y \cos \tilde{\epsilon} U_{i2}; \end{aligned} \quad (B2)$$

in the case of Dirac neutrinos. In the case of Majorana neutrinos, l_{i1} and k_{i1} have to be multiplied by $1 = \frac{p_-}{2}$ or $i = \frac{p_-}{2}$ for the cases that $\tilde{\nu}_1$ is either the scalar state or the pseudo-scalar state, respectively. The total width is given by

$$(\tilde{t}_1 \rightarrow b^+ \tilde{\nu}_1) = \frac{1}{16m_{\tilde{t}_1} (2\pi)^5} \int \frac{d^3 p_b d^3 p_l}{E_b E_l} \frac{(E_{\tilde{t}_1} - E_b - E_l - E_{\tilde{\nu}_1})}{E_{\tilde{\nu}_1}} |T_{fi}|^2; \quad (B3)$$

with

$$E_{\tilde{\nu}_1} = \sqrt{m_{\tilde{\nu}_1}^2 + (\mathbf{p}_{\tilde{t}_1} - \mathbf{p}_b - \mathbf{p}_l)^2}; \quad (B4)$$

$$|T_{fi}|^2 = \sum_{i=1/2}^X \frac{|T_{rii}|^2}{(\mathbf{p}_{\tilde{t}_1} - \mathbf{p}_b)^2 m_{\tilde{\nu}_1^+}^2} + 2 \text{Re} \left[\frac{T_{r12}}{(\mathbf{p}_{\tilde{t}_1} - \mathbf{p}_b)^2 m_{\tilde{\nu}_1^+}^2 (\mathbf{p}_{\tilde{t}_1} - \mathbf{p}_l)^2 m_{\tilde{\nu}_2^+}^2} \right]; \quad (B5)$$

$$\begin{aligned} T_{rii} &= 2 [k_{i1}^t]^2 [k_{i1}]^2 + [l_{i1}^t]^2 [l_{i1}]^2 - 2(\mathbf{p}_{\tilde{t}_1} - \mathbf{p}_b) \cdot \mathbf{p} (\mathbf{p}_{\tilde{t}_1} - \mathbf{p}_l) \cdot \mathbf{p} (\mathbf{p}_{\tilde{t}_1} - \mathbf{p}_b)^2 p_b \cdot \mathbf{p} \\ &+ 2m_{\tilde{\nu}_1^+}^2 [k_{i1}^t]^2 [l_{i1}]^2 + [l_{i1}^t]^2 [k_{i1}]^2 \mathbf{p} \cdot \mathbf{p} \\ &+ 4m_b m_{\tilde{\nu}_1^+} \text{Re}(k_{i1}^t l_{i1}^t) [l_{i1}]^2 + [k_{i1}]^2 (\mathbf{p}_{\tilde{t}_1} - \mathbf{p}_b) \cdot \mathbf{p} \\ &+ 4m_b m_{\tilde{\nu}_1^+} \text{Re}(k_{i1} l_{i1}^t) [l_{i1}^t]^2 + [k_{i1}^t]^2 (\mathbf{p}_{\tilde{t}_1} - \mathbf{p}_b) \cdot \mathbf{p} \\ &+ 4m_b m_{\tilde{\nu}_1^+} \text{Re}(k_{i1}^t k_{i1} l_{i1} l_{i1}^t) (\mathbf{p}_{\tilde{t}_1} - \mathbf{p}_b) \cdot (\mathbf{p} - \mathbf{p}_b) + m_{\tilde{\nu}_1^+}^2; \end{aligned} \quad (B6)$$

$$\begin{aligned} T_{r12} &= 2 [k_{11}^t k_{11} k_{21} k_{21}^t + l_{11}^t l_{11} l_{21} l_{21}^t] \\ &- 2(\mathbf{p}_{\tilde{t}_1} - \mathbf{p}_b) \cdot \mathbf{p} (\mathbf{p}_{\tilde{t}_1} - \mathbf{p}_l) \cdot \mathbf{p} (\mathbf{p}_{\tilde{t}_1} - \mathbf{p}_b)^2 p_b \cdot \mathbf{p} \\ &+ 2m_{\tilde{\nu}_1^+} m_{\tilde{\nu}_2^+} [k_{11}^t l_{11} l_{21} k_{21}^t + l_{11}^t k_{11} l_{21}^t k_{21}] \mathbf{p} \cdot \mathbf{p} \end{aligned}$$

$$\begin{aligned}
& + 2m_b m_{\tilde{\nu}_1^+} k_{11}^t l_{11} l_{21} l_{21}^t + l_{11}^t k_{11} k_{21} k_{21}^t (p_{t_1} - p) \\
& + 2m_{\tilde{\nu}_2^+} m_b k_{11}^t k_{11} l_{21}^t k_{21} + l_{11}^t l_{11} l_{21} k_{21}^t (p_{t_1} - p) \\
& 2m m_{\tilde{\nu}_1^+} k_{11}^t l_{11} k_{21} k_{21}^t + l_{11}^t k_{11} l_{21} l_{21}^t (p_{t_1} - p) \\
& 2m_{\tilde{\nu}_2^+} m k_{11}^t k_{11} l_{21} k_{21}^t + l_{11}^t l_{11} l_{21}^t k_{21} (p_{t_1} - p) \\
& 2m m_b k_{11}^t k_{11} l_{21} l_{21}^t + l_{11}^t l_{11} k_{21} k_{21}^t (p_{t_1} - p) \\
& 2m_{\tilde{\nu}_2^+} m m_b m_{\tilde{\nu}_1^+} k_{11}^t l_{11} l_{21}^t k_{21} + l_{11}^t k_{11} l_{21} k_{21}^t : \tag{B 7}
\end{aligned}$$

- [1] P. Minkowski, Phys. Lett. B 67, 421 (1977); M. Gell-Mann, P. Ramond, and R. Slansky, "Complex Spinors and Unified Theories", Proceedings of the Workshop, Stony Brook, New York, North-Holland, 1979; T. Yanagida, (KEK, Tsukuba), 1979; R. N. Mohapatra and G. Senjanovic, Phys. Rev. Lett. 44, 912 (1980).
- [2] For recent, complete reviews (and many references), see A. de Gouvêa, [hep-ph/0411274]; A. Strumia and F. Vissani, [hep-ph/0606054].
- [3] G. A. Blair, W. Porod and P. M. Zerwas, Eur. Phys. J. C 27, 263 (2003) [hep-ph/0210058]; A. Freitas, W. Porod and P. M. Zerwas, Phys. Rev. D 72, 115002 (2005) [hep-ph/0509056]; M. R. Buckley and H. Murayama, [hep-ph/0606088].
- [4] A. de Gouvêa, Phys. Rev. D 72, 033005 (2005) [hep-ph/0501039].
- [5] S. Gopalakrishna, A. de Gouvêa and W. Porod, JCAP 0605, 005 (2006) [hep-ph/0602027].
- [6] T. Asaka, K. Ishiwata and T. Moroi, [hep-ph/0512118].
- [7] J. S. Hagelin, G. L. Kane and S. Raby, Nucl. Phys. B 241, 638 (1984); L. J. Hall, T. Moroi and H. Murayama, Phys. Lett. B 424, 305 (1998) [hep-ph/9712515]; S. Kolb, M. Hirsch, H. V. Klapdor-Kleingrothaus and O. Panella, Phys. Lett. B 478, 262 (2000) [hep-ph/9910542]; N. Arkani-Hamed, L. J. Hall, H. Murayama, D. R. Smith and N. Weiner, Phys. Rev. D 64, 115011 (2001) [hep-ph/0006312]; C. L. Chou, H. L. Lai and C. P. Yuan, Phys. Lett. B 489, 163 (2000) [hep-ph/0006313].
- [8] C. L. Chou and M. E. Peskin, Phys. Rev. D 61, 055004 (2000) [hep-ph/9909536];
- [9] See for example, J. L. Feng and T. Moroi, Phys. Rev. D 58, 035001 (1998) [hep-ph/9712499]; G. F. Giudice and R. Rattazzi, Phys. Rept. 322, 419 (1999) [hep-ph/9801271].

- [10] See for example, J. R. Ellis and S. Rudaz, Phys. Lett. B 128, 248 (1983); V. D. Barger, M. S. Berger and P. Ohm ann, Phys. Rev. D 49, 4908 (1994) [hep-ph/9311269]; A. D juadi, J. Kalinowski, P. Ohm ann and P. M. Zerwas, Z. Phys. C 74, 93 (1997) [hep-ph/9605339].
- [11] See for example, M. Carena, M. Quiros and C. E. M. Wagner, Phys. Lett. B 380, 81 (1996) [hep-ph/9603420]; M. Quiros, Nucl. Phys. Proc. Suppl. 101, 401 (2001) [hep-ph/0101230]; M. Carena, M. Quiros, M. Seco and C. E. M. Wagner, Nucl. Phys. B 650, 24 (2003) [hep-ph/0208043].
- [12] W. Porod and T. W ohm ann, Phys. Rev. D 55 (1997) 2907 [Erratum ~~ibid.~~ D 67 (2003) 059902] [hep-ph/9608472]; W. Porod, Phys. Rev. D 59, 095009 (1999) [hep-ph/9812230]; C. Boehm, A. D juadi and Y. M am brini, Phys. Rev. D 61 (2000) 095006 [hep-ph/9907428]; R. Dem ina, J. D. Lykken, K. T. M atchev and A. Nom erotski, Phys. Rev. D 62, 035011 (2000) [hep-ph/9910275]; A. D juadi, M. G uchait and Y. M am brini, Phys. Rev. D 64 (2001) 095014 [hep-ph/0105108]; S. P. Das, A. Datta and M. G uchait, Phys. Rev. D 65 (2002) 095006 [hep-ph/0112182]; M. Carena, D. Choudhury, R. A. D iaz, H. E. Logan and C. E. M. Wagner, Phys. Rev. D 66, 115010 (2002) [hep-ph/0206167].
- [13] B. C. Allanach et al., [hep-ph/0602198].
- [14] T. Sjstrand, P. Eden, C. Friberg, L. Lonnblad, G. M iu, S. M renna and E. Norrbin, Computer Physics Commun. 135 (2001) 238; T. Sjstrand, L. Lonnblad, S. M renna and P. Skands, [hep-ph/0308153].
- [15] See, for example, A. C. Kraan, Eur. Phys. J. C 37, 91 (2004) [hep-ex/0404001]; W. Kilian, T. Plehn, P. Richardson and E. Schmidt, Eur. Phys. J. C 39, 229 (2005) [hep-ph/0408088]; J. L. Hewett, B. Lillie, M. Masip and T. G. R izzo, JHEP 0409, 070 (2004) [hep-ph/0408248]; A. C. Kraan, J. B. Hansen and P. Nevski, hep-ex/0511014.
- [16] For a recent discussion (in a rather different context), see K. Cheung and W. Y. Keung, Phys. Rev. D 71, 015015 (2005) [hep-ph/0408335].
- [17] C. R. Nappi, Phys. Rev. D 25, 84 (1982). For collider studies see, for example, P. M oxhay and R. W. Robinett, Phys. Rev. D 32, 300 (1985); M. J. Herrero, A. M endez and T. G. R izzo, Phys. Lett. B 200, 205 (1988); T. G. R izzo, Phys. Rev. D 40, 2803 (1989); V. D. Barger and W. Y. Keung, Phys. Lett. B 211, 355 (1988); M. D rees and M. M. No jiri, Phys. Rev. Lett. 72, 2324 (1994) [hep-ph/9310209]; M. D rees and M. M. No jiri, Phys. Rev. D 49, 4595 (1994) [hep-ph/9312213].

- [18] V. D. Barger, J. Ohnemus and R. J. N. Phillips, *Int. J. Mod. Phys. A* **4**, 617 (1989).
- [19] G. L. Kane, G. A. Ladinsky and C. P. Yuan, *Phys. Rev. D* **45**, 124 (1992); T. Stelzer and S. Willenbrock, *Phys. Lett. B* **374**, 169 (1996) [[hep-ph/9512292](#)]; D. Chang, S. C. Lee and A. Sumarokov, *Phys. Rev. Lett.* **77**, 1218 (1996) [[hep-ph/9512417](#)]; W. Bernreuther, A. Brandenburg, Z. G. Si and P. Uwer, *Nucl. Phys. B* **690**, 81 (2004) [[hep-ph/0403035](#)]; For an ATLAS study, see for example, K. Smolek and V. Simak, ATLAS-PHYS-2003-012 (2003).
- [20] See for example W. Beenakker, M. Kramer, T. Plehn, M. Spira and P. M. Zerwas, *Nucl. Phys. B* **515**, 3 (1998) [[hep-ph/9710451](#)], and references therein.
- [21] S. Hesselbach, F. Franke and H. Fraas, *Phys. Lett. B* **492**, 140 (2000) [[hep-ph/0007310](#)].
- [22] W. Porod, M. Hirsch, J. Romao and J. W. F. Valle, *Phys. Rev. D* **63**, 115004 (2001) [[hep-ph/0011248](#)]; F. de Campos, O. J. P. Eboli, M. B. Magro, W. Porod, D. Restrepo and J. W. F. Valle, *Phys. Rev. D* **71**, 075001 (2005) [[hep-ph/0501153](#)]; M. Hirsch, W. Porod and D. Restrepo, *JHEP* **0503**, 062 (2005) [[hep-ph/0503059](#)].
- [23] D. Acosta et al. [CDF Collaboration], *Phys. Rev. Lett.* **93**, 142001 (2004) [[hep-ex/0404036](#)]; V. M. Abazov et al. [D0 Collaboration], *Phys. Lett. B* **626**, 55 (2005) [[hep-ex/0505082](#)].
- [24] V. M. Abazov et al. [D0 Collaboration], D0-Notes 5050-CONF, 5039-CONF and 4866-CONF; A. A. Abolder et al. [CDF Collaboration], *Phys. Rev. Lett.* **84**, 5273 (2000) [[hep-ex/9912018](#)].
- [25] N. Kidonakis and R. Vogt, *Int. J. Mod. Phys. A* **20**, 3171 (2005) [[hep-ph/0410367](#)].
- [26] See, for example, A. de Gouvêa, A. Friedland and H. Murayama, *Phys. Rev. D* **59**, 095008 (1999) [[hep-ph/9803481](#)]; A. Datta, M. Guchait and N. Parua, *Phys. Lett. B* **395**, 54 (1997) [[hep-ph/9609413](#)].